Control of Stimulated Raman Scattering in the Strongly Nonlinear and Kinetic Regime Using Spike Trains of Uneven Duration and Delay

B. J. Albright,[1,*] L. Yin,[1] and B. Afeyan[2]
[1]Los Alamos National Laboratory, Los Alamos, New Mexico 87545, USA
[2]Polymath Research, Inc., Pleasanton, California 94566, USA
(Received 16 April 2013; revised manuscript received 6 May 2014; published 23 July 2014)

Stimulated Raman scattering (SRS) in its strongly nonlinear, kinetic regime is controlled by a technique of deterministic, strong temporal modulation and spatial scrambling of laser speckle patterns, called spike trains of uneven duration and delay (STUD) pulses [B. Afeyan and S. Hüller (unpublished)]. Kinetic simulations show that the proper use of STUD pulses decreases SRS reflectivity by more than an order of magnitude over random-phase-plate or induced-spatial-incoherence beams of the same average intensity and comparable bandwidth.

DOI: 10.1103/PhysRevLett.113.045002 PACS numbers: 52.35.Fp, 52.35.Mw, 52.38.Bv, 52.38.Dx

Laser-plasma instabilities (LPI) pose a risk to realizing laser-driven inertial confinement fusion (ICF) ignition [1]. The present approach is to use continuous, ns-time-scale illumination of a target with high-intensity laser beams. However, this may prove to be less than ideal when compared with a novel technique [2–4] employing intermittent, scintillating, space-time illumination which may significantly reduce levels of nonlinear optical processes. The efficacy of this spike trains of uneven duration and delay (STUD) pulses technique has been demonstrated in the fluid regime up to moderate gains per laser speckle, where cumulative growth is halted by the use of STUD pulses and saturation is from pump depletion [2–4]. Here we consider application of STUD pulses to stimulated Raman scattering (SRS) in settings where kinetic nonlinearity dominates the driven electron plasma waves (EPW) evolution and multi-laser-speckle, cooperative behavior proceeds through the exchange of hot electrons and SRS scattered light among speckles [5–7]. We find that order-of-magnitude reduction in SRS reflectivity is possible. The key is to keep SRS growth below levels where cooperative behavior among hot spots occurs, thus disallowing self-organization.

SRS is the resonant, three-wave coupling of a light wave into scattered light and EPW. At the National Ignition Facility (NIF), experiments show ~50% inner-cone beam energy loss to SRS [1]. To reduce LPI backscatter, laser facilities such as OMEGA and the NIF employ beam smoothing, whereby random phase plates (RPP) effect a quasiuniform (on the large scale) intensity across the beam though introducing small-scale, high-intensity variations or "speckles" [8]. In vacuum, speckles have size $4f^2\lambda_0$ (longitudinally) by $f\lambda_0$ (transversely), where f is the laser focal parameter and λ_0 is the wavelength. The scaling of SRS reflectivity R_{SRS} with laser intensity I in a solitary speckle in plasma has been measured [9] and found in the electron trapping regime $k\lambda_{\mathrm{De}} \gtrsim 0.3$ (k is the EPW wave number and $\lambda_{\mathrm{De}} = \sqrt{k_B T_e/4\pi n_e e^2}$ is the Debye length for plasma of electron density n_e and temperature T_e) to increase sharply at a threshold I_{th} and saturate for $I > I_{\mathrm{th}}$. The nonlinear physics in this regime is governed by large-amplitude EPW that trap resonant electrons with speeds along the wave propagation direction matching the wave's phase speed; this reduces Landau damping [10], and lowers the EPW frequency [11]. At high intensity, trapping introduces variation in EPW phase velocity across the speckle and the wave phase fronts bend [12–15]. As EPW grow, secondary, nonlinear processes may break the phase fronts into small-transverse-scale filaments [15–17] that further contribute to saturation. An effect of saturation [5] is the generation of hot electrons and back- and side-scattered light propagating out of hot spots and enhancing SRS growth in neighboring speckles through larger seed levels and reduced EPW damping. At high gain in two spatial dimensions, this coupling enables networks of speckles to exhibit collective behavior with reflectivity exceeding that of the sum of contributions from noninteracting speckles [5]. The nonlinear nature of SRS in this regime is robust, with a threshold at modest laser intensity, $\gtrsim 10^{14}\ \mathrm{W/cm^2}$ for NIF laser conditions where $k\lambda_{\mathrm{De}} \approx 0.3$ and the highest levels of backscatter are found [18].

The use of STUD pulses [2], effective for controlling LPI over long time scales in the fluid regime [2–4], may also inhibit EPW growth in the highly nonlinear, kinetic regime. STUD pulses deliver laser power in a sequence of pulses on the instability growth or hot spot crossing time scale with randomized speckle patterns in between one or more successive spikes. By introducing on-off sequences of pulses and by spatially scrambling locations of hot spots, reinforcing processes within a hot spot and the interconnectivity between hot spots are disrupted. STUD pulses introduce degrees of freedom that can be optimized [2]. These include the ratios $L_{\mathrm{HS}}:L_{\mathrm{INT}}:L_{\mathrm{spike}}$, where the interaction length is $L_{\mathrm{INT}} = 4L_n[\alpha^2 I_{14} + (\nu_2/\omega_2)^2]^{1/2}$, the density scale length is $L_n = |\nabla \log n_e|^{-1}$, I_{14} is intensity in 10^{14} W/cm^2, ν_2 and ω_2 are the local Landau damping rate and frequency of the EPW, respectively, $\alpha^2 = 1.14 \times 10^{-4} (\lambda_0^{[\mu m]})^2 |V_2/V_1| (n_e/n_{cr})^{-1}$, and V_2/V_1 is the ratio of group velocities of EPW to scattered SRS light [2]. Spike length L_{spike} is the distance traveled by scattered light during the "on" time τ_{spike} and $L_{HS} \sim 4f^2\lambda_0 = 90$ μm is the size of a hot spot (HS) in our plasma. Other degrees of freedom are duty cycle (ratio of τ_{spike} to on + off time), spatial scrambling rate $\times n_{scram}$ (how many spikes before the RPP pattern changes), and "jitter" (small random variations of each τ_{spike} to avoid low-frequency resonances [2]; because in the absence of ion motion or low frequency secondary waves SRS has no such resonances, the calculations here use 0% jitter). Hence, "5000×1, 1:0.5:0.5" indicates a STUD pulse sequence with 50% duty cycle, 0% jitter, and a spike half as long as a hot spot crossing time in plasma where the time to cross L_{INT} for the three-wave process is also half that of crossing the hot spot. Most of the results we present are for cases 5000×1, 1:0.5:0.5 and 1:0.5:1 in strong to very strong nonlinear kinetic regimes (SRS gains of 4–8.7 at the average intensity) [19]. Note that configurations where "on" time is much greater than "off" time, e.g., 8000×1 or 9500×1, resemble the induced-spatial-incoherence (ISI) model of beam smoothing [20] at the same bandwidth.

To explore STUD pulses in the trapping regime, we ran collisionless VPIC particle-in-cell simulations [21] of a two-dimensional plasma of size 500×80 μm in (x, z), with laser polarized along y launched at $x = 0$ as described in Ref. [6]. The laser has wavelength $\lambda_0 = 0.351$ μm and an RPP speckle pattern for $f\backslash 8$ speckles, approximating a NIF inner-cone beam. The density gradient along x has $n_e = 0.12 n_{cr}$ at the center, varying by $\pm 0.03 n_{cr}$ across the box, comparable to the $L_n \sim$ mm encountered in NIF ignition hohlraums in regions of high SRS backscatter [18]. Taking $\nu_2 = \nu_2^{Max}$, as for Maxwellian plasma, in the $k\lambda_{De} \approx 0.3$ regime yields $L_{INT} \sim 46$–52 μm for the intensities simulated. We use 36864×4096 cells ($\Delta x = 1.2\lambda_{De}$ and $\Delta z = 1.7\lambda_{De}$) and 256 electron macroparticles/cell; the ions are a stationary, neutralizing background [22]. The electrons have $T_e = 2.6$ keV ($k\lambda_{De} = 0.3$, $|\nu_2^{Max}/\omega_{pe}| = 0.015$). The STUD pulse speckle patterns are generated from pre-computed RPP phases for a wide beam, sampling 80-μm, nonoverlapping segments for each STUD pulse; such multispeckle VPIC simulations of SRS have been validated in experiments using the Jupiter laser [23]. Each simulation generated STUD pulses from an identical sequence of RPP speckle patterns on the boundaries, but with the STUD pulse intensity, duty cycle, and modulation period varied as per the STUD pulse prescription. (Statistical variation was assessed by altering the sequences of STUD pulses; $\sim$10% relative R_{SRS} variation was found in a range of cases considered.) The simulation boundaries absorb electromagnetic waves and reinject electrons as Maxwellian at initial temperature T_e. The simulations were run until apparent "steady-state" in time-averaged R_{SRS}, 10–20 ps. Time-averaged R_{SRS} values were computed by time-averaging the spatially integrated Poynting flux on the left simulation boundary after subtracting the incident laser Poynting flux, then dividing by the time-averaged, incident laser power over the duration of the simulation.

Fig. 1 shows a comparison of three simulations: (a) (top row) is for an RPP beam with $\langle I \rangle = 5 \times 10^{14}$ W/cm^2 ($G = 8.7$); (c) (bottom) is for a STUD pulse beam of time-averaged intensity $\langle I \rangle = 3.2 \times 10^{14}$ W/cm^2 ($G = 5.6$). Linear SRS gains G are computed from $G = 4\pi(\gamma_0/\omega_0)^2 (2\pi L_n/\lambda_0) g^{-1} (1 - \nu_1\nu_2/\gamma_0^2)$, where $(\gamma_0/\omega_0) = 0.0043\sqrt{I_{14}}\lambda_0^{[\mu m]}$, ν_1 is the damping rate of the daughter light wave, and $g(n) \equiv \sqrt{1 - 2\sqrt{n}}[(1/\sqrt{n}) - 1]^{-1}$, with density n normalized to the critical density [2]. Accounting for backscatter, (a) and (c) have comparable net time-averaged power injected on the left boundary, though (c) has only 64% of the incident time-averaged laser power. Case (b) (center) is for a STUD pulse beam at the same time-averaged incident laser intensity as (a): $\langle I \rangle = 5 \times 10^{14}$ W/cm^2 ($G = 8.7$). The leftmost panels show E_y (or the vacuum speckle pattern for the RPP case). The

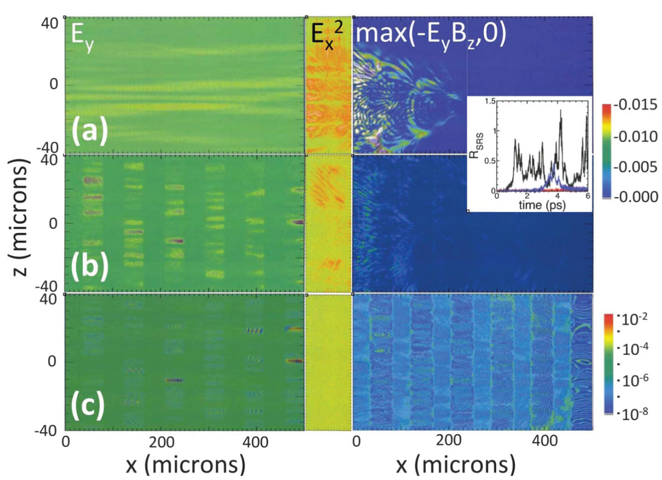

FIG. 1 (color). E_y (left) and corresponding instantaneous backscattered Poynting flux $\max(-E_yB_z, 0)$ (right) over the two-dimensional simulation volume for cases: (a) an RPP laser beam at average laser intensity $\langle I \rangle = 5 \times 10^{14}$ W/cm^2 (top), (b) a 5000×1, 1:0.5:0.5 STUD pulse beam at time-averaged incident laser intensity $\langle I \rangle = 5 \times 10^{14}$ W/cm^2 (center); and, (c) the same STUD pulse beam, but with $\langle I \rangle = 3.2 \times 10^{14}$W/cm^2 (bottom) (note logarithmic scale on Poynting flux). The center panels are E_x^2 for the leftmost 80 μm of each simulation, showing EPW wave amplitude correlated with instantaneous SRS backscattered Poynting flux. The inset is reflectivity vs time for cases (a) (black) and (b) (blue); (c) (red) evinces negligible backscatter. The times shown are 1.6 ps (a) and 3.6 ps (b),(c), chosen when large, bursts of SRS backscatter were present in (a) and (b).

rightmost panels are backscattered Poynting flux $\max(-E_y B_z, 0)$. Case (a) evinces continual bursts of self-organized backscatter with peak $R_{\mathrm{SRS}} > 1$. In (c), no self-organization is seen in backscattered light or longitudinal electric field. Case (b) is intermediate, with quiescent periods of low backscatter and occasional episodes of partial self-organization when large-amplitude speckles ($I \gtrsim 10\langle I\rangle$) have large-amplitude EPW and secondary processes, such as obliquely side-scattered light, occur at sufficient amplitude to seed SRS in otherwise stable regions of plasma (seen in the finite backscattered SRS Poynting flux across the left of the box). The instantaneous R_{SRS} at the left boundary for (a–c) is shown in the inset; the times plotted are 1.6 ps for the RPP (during the first large SRS burst), and 3.6 ps for the STUD pulse simulations [during the first, large SRS burst in (b)]. The central panels are E_x^2 over the leftmost 80 μm of the volume and indicate EPW correlated with large bursts of SRS in (a) and (b).

In Fig. 2, we compare for (a)–(c) time-integrated hot electron flux per unit area exiting the simulation. The black curves are fluxes leaving the $\pm z$ boundaries from the left half of the simulation volume, the red curves, leaving $\pm z$ from the right of the volume, and the blue curves, leaving from the $+x$ boundary. Prior work showed that large fluxes of tail electrons leaving the left of the side boundaries (i.e., large black curves) indicate large-amplitude EPW with nonlinear self-focusing, filamentation, and collective behavior among speckles [6,7]. The three cases evince elevated distribution function tails as a consequence of trapping, though the RPP traps not only far more tail

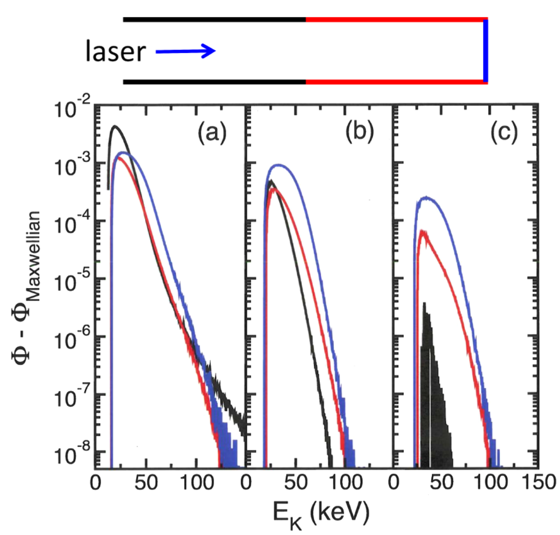

FIG. 2 (color online). Hot electron flux per unit length Φ vs electron energy (E_K) for the three simulations in Fig. 1. Shown are trapped particle fluxes, obtained by subtracting contributions from a Maxwellian (time-averaged over the duration of the simulation). Fluxes are measured on boundary regions, as indicated by the colors (c.f. the simulation box above, drawn to scale): $z = \pm 40$ μm, $0 < x < 250$ μm (black); $z = \pm 40$ μm, $250 < x < 500$ μm (red) and $x = 500$ μm (blue).

electrons [60× more than (c), 6× more than (b)], but also shows far more side-scattered hot electrons exiting nearest the laser entrance; moreover, hot electrons at very high energy ($E_K > 100$ keV) are present (absent for the STUD pulse beams). The use of STUD pulses has decreased the number of hot electrons exchanged laterally among laser speckles, key to interspeckle self-organization [7] and a possible contributor to capsule preheat in ICF experiments. In Fig. 3, we compare angular spread of SRS scattered light. The use of STUD pulses dramatically reduces SRS power (and hence, amplitude of the SRS seed in neighboring speckles). As with the RPP, the angular spread is finite, with most of the power falling outside the incident laser cone $|\theta| < 1/2f$ shown by the vertical lines. While the coherent, oblique cones of backscattered light are not unique to this regime (they appear in paraxial models with diffraction [2,24]) additional side-scatter results from trapping and EPW filamentation [5,17] absent in fluid models; the use of STUD pulses reduces these side-scatter levels.

Finally, in Fig. 4, we compare the dependence of R_{SRS} on time-averaged incident laser intensity (left) and linear gain at the average intensity (right) for RPP and STUD pulses. STUD pulses reduce R_{SRS} compared with RPP and ISI-like beams with the same time-averaged laser power even in cases of high linear gain. As seen from comparison of the R_{SRS} from the ISI-like points (the 8000×1, $1{:}0.5{:}0.5$ and 9500×1, $1{:}0.5{:}0.5$) and 5000×1, $1{:}0.5{:}0.5$ cases, "healing time" is key: it is not enough to simply add bandwidth and spatial scrambling. By optimizing this healing time for given on + off time and time-averaged power, STUD pulses may be fashioned to significantly outperform ISI. From comparison of the 5000×4, $1{:}0.5{:}0.5$ and the 5000×1, $1{:}0.5{:}0.5$ cases, we find that spatial scrambling of the hot spot locations is also necessary to minimize recurrence and correlation among hot

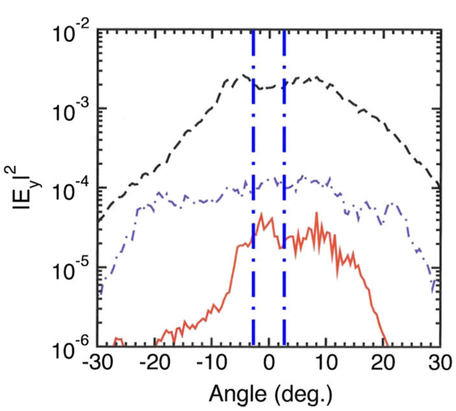

FIG. 3 (color online). Angular distribution of the time-averaged backscattered light power for cases (a) (black, dashed), (b) (dot-dashed, blue), and (c) (red) as in Figs. 1 and 2. The spectra for (b) and (c) evince lower backscattered light power, but finite angle with respect to the incident laser (cone angle $|\theta| < 1/2f$, shown by the vertical lines).

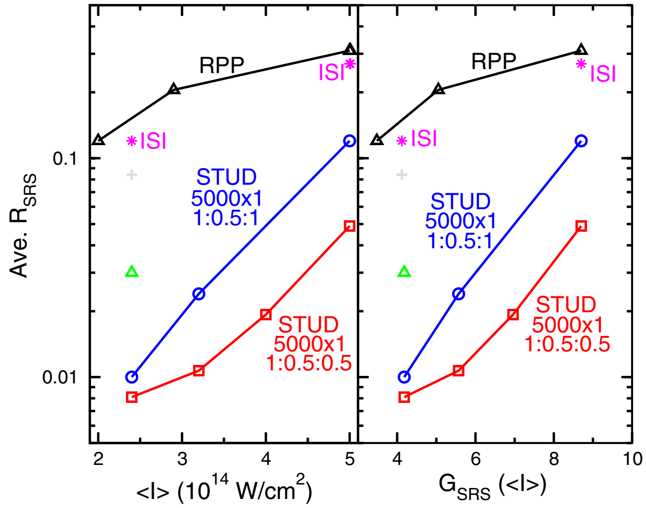

FIG. 4 (color online). SRS reflectivity vs average incident intensity (left) and linear gain (right) for RPP and a variety of STUD-pulse beams. The black (△) are for RPP. Red (□) and blue (∘) curves are for STUD pulses with 5000×1, $1{:}0.5{:}0.5$ and 5000×1, $1{:}0.5{:}1$ (i.e., twice the "on" time) for the latter density profile. The magenta points labeled "ISI" are for STUD pulses with 8000×1, $1{:}0.5{:}0.5$ (left) and 9500×1, $1{:}0.5{:}0.5$ (right) and indicate little advantage over RPP for the conditions shown. The green (△) is for STUD pulses with 5000×4, $1{:}0.5{:}0.5$, i.e., scrambling every four pulses. The (+) is for 2000×1, $1{:}0.5{:}0.5$.

spots. Also, for fixed on + off time and time-averaged power, lengthening the off time requires shortening τ_{spike} and increasing average speckle intensity correspondingly. Taken to an extreme, this can enhance trapping and associated EPW nonlinearity, evinced by the 2000×1 datum in Fig. 4 [which also has significant hot electron sidescatter (not shown) compared with the 5000×1, $1{:}0.5{:}0.5$ case at the same average power]. Incidentally, because of how geometry affects speckle coupling, cross-speckle coupling through SRS side-loss hot electrons is lower in three dimensions vs two dimensions [7] and the probability of spatial recurrence of hot spots is smaller in three dimensions. Consequently, advantages of STUD pulses in the nonlinear, kinetic regime of SRS should be more pronounced in three dimensions.

Examination of velocity distribution functions and EPW amplitudes shows strong trapping and only modest EPW damping between pulses. This trapping modifies L_{INT} and suggests possible threshold behavior when $L_{\text{INT}} > L_{\text{spike}}$ and SRS goes from strong to weak damping. Consider the two 5000×1 STUD pulse cases at the highest intensity ($G = 8.7$). In the former, SRS in the largest amplitude hot spots ($I \gtrsim 10\langle I \rangle$) would be in the weak damping limit if one were to apply the inferred ν_2 from simulations ($\approx 0.1\nu_2^{\text{Max}}$), and $L_{\text{INT}} \approx 84\ \mu$m. The $1{:}0.5{:}0.5$ case, with the lowest R_{SRS}, has $L_{\text{spike}} = 0.56 L_{\text{INT}}$ for these maximal speckles, so STUD pulses effectively shorten the interaction length. In contrast, the $1{:}0.5{:}1$ case has (effectively) no such reduction ($L_{\text{spike}} \sim L_{\text{INT}}$) and only exhibits a modest (~2×) reduction in R_{SRS}.

We have shown that SRS reflectivity may be lowered by an order of magnitude with the use of properly designed STUD pulses when EPW trapping-induced nonlinearity is prevalent. This reduction stems from arresting large-amplitude EPW leading to cooperative behavior among laser speckles through the exchange of hot electrons and backscatter SRS waves. Relative to what we have explored here, two complications arise in realizing these advantages in ICF experiments. (1) The largest reduction of SRS in our study for $f\backslash 8$ speckles required very short pulses and high laser bandwidth (> 3.3 THz for 0.3 ps "on + off" pulse duration), inaccessible on existing ICF lasers (however, if the laser were $f\backslash 20$ as for current NIF beams, then the hot spot traversal time would be 2 ps, and 1 ps STUD pulse modulations (THz) would cut speckles in half and thus may be sufficient to suppress SRS). (2) As found from additional simulations (not shown), the reduction in R_{SRS} depends on density scale length along the direction of laser propagation, determined by hydrodynamic evolution of the plasma. Achieving optimal STUD pulses in such a setting would require adapting the train of pulses to respond to the changing profiles, a point that has been identified as a key feature of STUD pulses [2].

Work conducted under the auspices of the NNSA of the U.S. Department of Energy at Los Alamos National Laboratory, managed by LANS, LLC, under Contract No. DE-AC52-06NA25396. B. J. A. and L. Y. were supported by DOE NNSA ICF and LDRD Programs and the DOE NNSA-OFES Joint program in HEDLP. B. A. was supported by grants from the DOE NNSA-OFES Joint program in HEDLP and by SBIR grants from OFES. Simulations were performed on ASC Roadrunner and Cielo. We acknowledge useful discussions with S. Hüller, J. Garnier, J. Fernández, D. Montgomery, J. Kline, and S. Batha.

*balbright@lanl.gov

[1] William Goldstein and Robert Rosner, *Proceedings of Science Fusion Ignition on NIF Workshop, LLNL-TR-570412, San Ramon, CA, 2012* (Lawrence Livermore National Laboratory, Livermore, 2012); William L. Kruer, in *Laser-Plasma Interactions and Applications*, Scottish Graduate Series, edited by P. McKenna *et al.* (Springer, Berlin, 2013).
[2] B. Afeyan and S. Hüller, arXiv:1304.3960.
[3] B. Afeyan and S. Hüller, Eur. Phys. J. **59**, 05009 (2013).
[4] S. Hüller and B. Afeyan, Eur. Phys. J. **59**, 05010 (2013).
[5] L. Yin, B. J. Albright, H. A. Rose, K. J. Bowers, B. Bergen, and R. K. Kirkwood, Phys. Rev. Lett. **108**, 245004 (2012).
[6] L. Yin *et al.*, Phys. Plasmas **19**, 056304 (2012).

[7] L. Yin, B. J. Albright, H. A. Rose, D. S. Montgomery, J. L. Kline, R. K. Kirkwood, P. Michel, K. J. Bowers, and B. Bergen, Phys. Plasmas **20**, 012702 (2013).

[8] J. D. Moody, B. MacGowan, J. Rothenberg, R. Berger, L. Divol, S. Glenzer, R. Kirkwood, E. Williams, and P. Young, Phys. Rev. Lett. **86**, 2810 (2001).

[9] D. S. Montgomery, J. A. Cobble, J. C. Fernández, R. J. Focia, R. P. Johnson, N. Renard-LeGalloudec, H. A. Rose, and D. A. Russell, Phys. Plasmas **9**, 2311 (2002).

[10] T. O'Neil, Phys. Fluids **8**, 2255 (1965).

[11] G. J. Morales and T. M. O'Neil, Phys. Rev. Lett. **28**, 417 (1972).

[12] L. Yin, B. J. Albright, K. J. Bowers, W. Daughton, and H. A. Rose, Phys. Rev. Lett. **99**, 265004 (2007).

[13] L. Yin, B. J. Albright, H. A. Rose, K. J. Bowers, B. Bergen, D. S. Montgomery, J. L. Kline, and J. C. Fernández, Phys. Plasmas **16**, 113101 (2009).

[14] J. W. Banks, R. L. Berger, S. Brunner, B. I. Cohen, and J. A. F. Hittinger, Phys. Plasmas **18**, 052102 (2011).

[15] C. Rousseaux, S. Baton, D. Bénisti, L. Gremillet, J. Adam, A. Héron, D. Strozzi, and F. Amiranoff, Phys. Rev. Lett. **102**, 185003 (2009).

[16] H. A. Rose, Phys. Plasmas **12**, 012318 (2005); H. A. Rose and L. Yin, Phys. Plasmas **15**, 042311 (2008).

[17] P. E. Masson-Laborde, W. Rozmus, Z. Peng, D. Pesme, S. Hüller, M. Casanova, V. Yu. Bychenkov, T. Chapman, and P. Loiseau, Phys. Plasmas **17**, 092704 (2010).

[18] R. K. Kirkwood *et al.*, Phys. Plasmas **18**, 056311 (2011); D. E. Hinkel *et al.*, Phys. Plasmas **18**, 056312 (2011); S. H. Glenzer *et al.*, Phys. Rev. Lett. **106**, 085004 (2011); R. K. Kirkwood *et al.*, Plasma Phys. Controlled Fusion **55**, 103001 (2013).

[19] During revision, we were made aware of an error in our calculations such that they were run outside the optimal $L_{\rm spike} = \min(L_{\rm HS}, L_{\rm INT})/2$ condition found by Afeyan and Hüller [2]. Repeating our calculations for these conditions may further reduce Raman backscatter.

[20] S. P. Obenschain *et al.*, Phys. Rev. Lett. **56**, 2807 (1986); R. Lehmberg and J. Rothenberg, J. Appl. Phys. **87**, 1012 (2000).

[21] K. J. Bowers, B. J. Albright, L. Yin, B. Bergen, and T. J. T. Kwan, Phys. Plasmas **15**, 055703 (2008); K. J. Bowers, B. J. Albright, B. Bergen, L. Yin, K. J. Barker, and D. J. Kerbyson, *Proceedings of the ACM/IEEE Conference on Supercomputing, Austin, 2008* (IEEE Press, Piscataway, NJ, 2008), p. 1; K. J. Bowers, B. J. Albright, L. Yin, W. Daughton, V. Roytershteyn, B. Bergen, and T. J. T. Kwan, J. Phys. Conf. Ser. **180**, 012055 (2009).

[22] This simplification stems from the restricted focus of this work on nonlinear SRS in the kinetic regime. In a more complete treatment of this problem, ions are mobile and Langmuir decay instability (LDI) is theoretically possible (though our simulations with mobile ions have not shown significant LDI at $k\lambda_{\rm De} \geq 0.3$). With immobile ions, we do not require the start-time randomization and use of jitter as in Ref. [2]. Moreover, the classical inverse bremsstrahlung absorption fraction of the laser and scattered light across the volume is $f_0 = 1 - \exp(-\kappa \cdot 500\ \mu{\rm m}) = 0.05$ and $f_1 = 0.18$, respectively, suggesting that inclusion of electron-ion collisions would be a minor correction.

[23] R. K. Kirkwood *et al.*, J. Plasma Phys. **77**, 521 (2011).

[24] T. Kolber, W. Rozmus, and V. T. Tikhonchuk, Phys. Fluids B **5**, 138 (1993).